

**AEDC-TR-85-62**

C.1

**ARCHIVE COPY  
DO NOT LOAN**

## **A Nonperturbing Boundary-Layer Transition Detector**

J. E. O'Hare  
Calspan Corporation

**PROPERTY OF U.S. AIR FORCE  
AEDC TECHNICAL LIBRARY**

**November 1985**

**Final Report for Period October 1983 — September 1985**

**TECHNICAL REPORTS  
FILE COPY**

Approved for public release; distribution unlimited.

**ARNOLD ENGINEERING DEVELOPMENT CENTER  
ARNOLD AIR FORCE STATION, TENNESSEE  
AIR FORCE SYSTEMS COMMAND  
UNITED STATES AIR FORCE**



AEDC TECHNICAL LIBRARY



1552 5E000 0220 5

## NOTICES

When U. S. Government drawings, specifications, or other data are used for any purpose other than a definitely related Government procurement operation, the Government thereby incurs no responsibility nor any obligation whatsoever, and the fact that the government may have formulated, furnished, or in any way supplied the said drawings, specifications, or other data, is not to be regarded by implication or otherwise, or in any manner licensing the holder or any other person or corporation, or conveying any rights or permission to manufacture, use, or sell any patented invention that may in any way be related thereto.

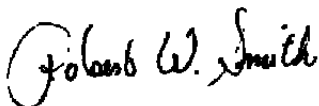
Qualified users may obtain copies of this report from the Defense Technical Information Center.

References to named commercial products in this report are not to be considered in any sense as an endorsement of the product by the United States Air Force or the Government.

This report has been reviewed by the Office of Public Affairs (PA) and is releasable to the National Technical Information Service (NTIS). At NTIS, it will be available to the general public, including foreign nations.

## APPROVAL STATEMENT

This report has been reviewed and approved.



ROBERT W. SMITH  
Directorate of Technology  
Deputy for Operations

Approved for publication:

FOR THE COMMANDER



LOWELL C. KEEL, Lt Colonel, USAF  
Director of Technology  
Deputy for Operations

UNCLASSIFIED

SECURITY CLASSIFICATION OF THIS PAGE

REPORT DOCUMENTATION PAGE				
1a. REPORT SECURITY CLASSIFICATION <b>UNCLASSIFIED</b>		1b. RESTRICTIVE MARKINGS		
2a. SECURITY CLASSIFICATION AUTHORITY		3. DISTRIBUTION/AVAILABILITY OF REPORT		
2b. DECLASSIFICATION/DOWNGRADING SCHEDULE		See Reverse of This Page		
4. PERFORMING ORGANIZATION REPORT NUMBER(S) <b>AEDC-TR-85-62</b>		5. MONITORING ORGANIZATION REPORT NUMBER(S)		
6a. NAME OF PERFORMING ORGANIZATION <b>Arnold Engineering Development Center</b>	6b. OFFICE SYMBOL (If applicable) <b>DOT</b>	7a. NAME OF MONITORING ORGANIZATION		
6c. ADDRESS (City, State and ZIP Code) <b>Air Force Systems Command Arnold Air Force Station, TN 37389-5000</b>		7b. ADDRESS (City, State and ZIP Code)		
8a. NAME OF FUNDING/SPONSORING ORGANIZATION <b>Arnold Engineering Development Center</b>	8b. OFFICE SYMBOL (If applicable) <b>DOT</b>	9. PROCUREMENT INSTRUMENT IDENTIFICATION NUMBER		
8c. ADDRESS (City, State and ZIP Code) <b>Air Force System Command Arnold Air Force Station, TN 37389-5000</b>		10. SOURCE OF FUNDING NOS		
		PROGRAM ELEMENT NO <b>065807F</b>	PROJECT NO <b>D228</b>	TASK NO <b>(V32L-B2)</b>
11. TITLE (Include Security Classification) <b>See Reverse of This Page</b>		WORK UNIT NO		
12. PERSONAL AUTHOR(S) <b>O'Hare, J. E., Calspan Corporation/AEDC Division</b>				
13a. TYPE OF REPORT <b>Final</b>	13b. TIME COVERED <b>FROM 10/83 TO 9/85</b>	14. DATE OF REPORT (Yr., Mo., Day) <b>November 1985</b>	15. PAGE COUNT <b>26</b>	
16. SUPPLEMENTARY NOTATION <b>Available in Defense Technical Information Center (DTIC).</b>				
17. COSATI CODES		18. SUBJECT TERMS (Continue on reverse if necessary; and identify by block number)		
FIELD <b>20</b>	GROUP <b>04</b>	SUB GR		
		lasers wind tunnel test		
		interferometry boundary-layer transition		
		measuring instruments		
19. ABSTRACT (Continue on reverse if necessary and identify by block number) A laser interferometer technique is being applied to the characterization of boundary-layer conditions on models in supersonic and hypersonic wind tunnels in the von Karman Facility at Arnold Engineering Development Center (AEDC). The boundary-layer transition detector (BLTD), based on lateral interferometry, is applicable for determining the turbulence frequency spectrum of boundary layers in compressible flow. The turbulence, in terms of air density fluctuations, is detected by monitoring interferometric fringe phase shifts (in real time) formed by one beam which passes through the boundary layer and a reference beam which is outside the boundary layer. This technique is nonintrusive to the flow field unlike other commonly used methods such as pitot tube probing and hot-wire anemometry. Data which depict boundary-layer transition from laminar to turbulent flow are presented to provide comparisons of the BLTD with other measurement methods.				
20. DISTRIBUTION/AVAILABILITY OF ABSTRACT <b>UNCLASSIFIED/UNLIMITED <input checked="" type="checkbox"/> SAME AS RPT <input type="checkbox"/> DTIC USERS <input type="checkbox"/></b>		21. ABSTRACT SECURITY CLASSIFICATION <b>UNCLASSIFIED</b>		
22a. NAME OF RESPONSIBLE INDIVIDUAL <b>W. O. Cole</b>		22b. TELEPHONE NUMBER (Include Area Code) <b>(615) 454-7813</b>	22c. OFFICE SYMBOL <b>DOS</b>	

DD FORM 1473, 83 APR

EDITION OF 1 JAN 73 IS OBSOLETE

UNCLASSIFIED  
SECURITY CLASSIFICATION OF THIS PAGE

UNCLASSIFIED

SECURITY CLASSIFICATION OF THIS PAGE

3. DISTRIBUTION/AVAILABILITY OF REPORT

Approved for public release; distribution is unlimited.

11. TITLE

A Nonperturbing Boundary-Layer Transition Detector

19. ABSTRACT (Concluded)

Spectra from the BLTD reveals the presence of a high-frequency peak during transition which is characteristic of spectra obtained with hot wires. The BLTD is described along with operational requirements and limitations.

UNCLASSIFIED

SECURITY CLASSIFICATION OF THIS PAGE

## **PREFACE**

The work reported herein was performed by the Arnold Engineering Development Center (AEDC), Air Force Systems Command (AFSC). Work and analysis for this research were done under Air Force Project No. D228 (V32L-B2) by personnel of Calspan Corporation/AEDC Division, operating contractor of the aerospace flight dynamics testing facilities at AEDC, AFSC, Arnold Air Force Station, Tennessee. The support of the Air Force Project Managers, Mr. Marshall Kingery and Mr. Bobby Smith, AEDC/DOT, is much appreciated. The work was conducted from October 1983 to September 1985, and the manuscript was submitted for publication on September 24, 1985.

The author wishes to express his appreciation to Mr. W. L. Templeton, Mr. M. E. Pope, and Mr. S. G. Howard for their work on development of the signal processing and data display system.

## CONTENTS

	<u>Page</u>
1.0 INTRODUCTION .....	5
2.0 DESCRIPTION OF TECHNIQUE .....	5
2.1 Methodology .....	6
2.2 Description of Instrument .....	7
2.2.1 Laser Light Source .....	7
2.2.2 Receiving Optics .....	7
2.2.3 Optical Signal Detection .....	8
2.2.4 Signal Processing and Display .....	8
3.0 WIND TUNNEL EXPERIMENTS .....	9
3.1 Instrument Traversing Mount .....	9
3.2 Experiment Procedure .....	10
3.2.1 Boundary-Layer Characterization .....	10
3.2.2 Comparison of BLTD Data .....	10
4.0 CONCLUSIONS .....	11
REFERENCES .....	11

## ILLUSTRATIONS

### Figure

1. Schematic of Boundary-Layer Transition Detector .....	13
2. Boundary-Layer Transition Detector and Signal Conditioning Schematic .....	14
3. Boundary-Layer Transition Detector System Hardware .....	15
4. Boundary-Layer Transition Detector Optical Head and Data Recording System .....	16
5. Boundary-Layer Transition Detector and Cone Model Installed in AEDC Hypersonic Tunnel B .....	17
6. Shadowgram of Laminar, Transitional, and Fully Turbulent Boundary-Layer Flow .....	18
7. Boundary-Layer Survey, 7-deg Cone, Mach 8, $Re/ft\ 2.0 \times 10^6$ .....	19
8. Boundary-Layer Survey, 7-deg Cone, Mach 8, $Re/ft\ 3.0 \times 10^6$ .....	20
9. Comparison of BLTD and Hot-Wire Spectra, Mach 8, $Re/ft$ $2.0 \times 10^6$ , Station X = 13 .....	21
10. Boundary-Layer Transition on a 7-deg Cone at Mach 8 .....	22

## 1.0 INTRODUCTION

An important aspect of testing models in supersonic and hypersonic wind tunnels is the determination of whether the model boundary-layer flow is laminar, transitional, or fully turbulent. Without this determination, simulation of actual vehicle flight conditions cannot be achieved. Several measurement techniques provide useful information about the turbulence in boundary layers, but each has some disadvantages (Ref. 1). Probes that are physically placed in the boundary layer, such as hot-wire probes and pitot probes, perturb the flow field to some unknown degree, which often raises a question about the validity of the data. Since these probes must be much smaller than the boundary-layer thickness, which is very thin at supersonic velocities, they are quite fragile and vulnerable to flow contaminants. Surface sensors, such as acoustic and heat-flux gages, that are mounted in the model respond only to phenomena adjacent to the model surface and are required in large numbers to obtain data along the full length of a model. Shadowgrams of the flow field show qualitative characteristics of the boundary layer under most conditions but only after time required for photographic processing of the images. Oil-flow and sublimation techniques alter or roughen the model surface and may influence the boundary-layer conditions.

This report describes a new optical technique for characterizing turbulence which circumvents many of the disadvantages of the above methods. This technique is nonintrusive to the flow field, does not require special model preparation or instrumentation, and displays the boundary-layer turbulence data in real time.

## 2.0 DESCRIPTION OF TECHNIQUES

In selecting a nonintrusive technique for characterizing boundary-layer conditions on a model in highly automated continuous-flow wind tunnels, considerations other than using the best optical method played an important role in the final selection. The first design requirement was that the instrument must be easy to install on a wind tunnel and require little time to align and prepare for operation. This meant that the instrument must be small and portable, must remain in alignment under vibrational and varying thermal conditions, and must be contained in a single unit as opposed to a separate transmitter and receiver located on opposite sides of the tunnel. Secondly, it was not to interfere with other wind tunnel measurement systems that are used for standard instrumentation, and thirdly, the instrument must provide data on a real-time basis so that decisions can be made during tunnel operations based on the boundary-layer conditions.

The optical method selected is based on lateral interferometry using a laser for the light source (Ref. 2). The concept for the interferometer was to split the laser beam into two beams, routing one beam through the model boundary layer tangential to the model surface

(probe beam), and routing the other beam outside the boundary layer (reference beam) (Fig. 1). The two beams then converge at an angle  $\theta$  and form a fringe zone with a fringe period ( $\lambda_s$ ) given by

$$\lambda_s = \frac{\lambda}{2 \sin \theta/2}$$

Density variations along the paths of the two beams cause the fringes to move in the vertical direction. The probe beam is focused at the point at which it traverses the boundary layer so that small-scale density cells that pass through the beam at this point move all of the fringes in an undistorted fashion. On the other hand, density cells which are much smaller than the beam diameter, other than in the focal point area and in the collimated reference beam, may have little or no effect on the complete fringe pattern. Since the area of the slit (the detectable area) is <2 percent of the fringe pattern area, small density cells passing through the unfocused areas of the beams can go undetected behind the slit opening.

## 2.1 METHODOLOGY

The decision to probe the boundary layer tangentially rather than normal to the model surface was based on getting the maximum optical signal-to-noise ratio from the optical path length of the probe beam. Since the boundary-layer thickness on models in supersonic and hypersonic flow can be very thin (as little as 2 to 4 mm thick), it is advantageous to have the beam path length as long as possible through the measurement area. Probing the boundary layer perpendicular to the model surface will reduce the optical signal-to-noise ratio at the same time requiring higher sensitivity interferometry for detecting turbulence. Model surface preparations, which are usually undesirable, may also be required to provide a suitable diffuse surface.

Although detection of fringe movement in a plane of the fringe zone located on the opposite side of the wind tunnel from the transmitter is more desirable optically, it would require moving the slit and detector in alignment with the optical head. This mechanically complex arrangement is not desirable for large wind tunnels. Mounting components of an optical system on separate mounts also increases potential problems because of the vibrational environment around large wind tunnels. Therefore, the option chosen was to image the fringe plane with a receiving lens back into the transmitting package onto the slit and photodetector.



## 2.2 DESCRIPTION OF INSTRUMENT

An instrument was built to evaluate the technique in supersonic and hypersonic wind tunnels A, B, and C at the Arnold Engineering Development Center. These tunnels are from 1 to 1.65 m wide between test section optical ports, so a working distance of 1 m from the front of the instrument package to the tunnel centerline was provided. A variation of lateral interferometry was configured to meet both the optical requirements and other operational requirements that have been outlined.

### 2.2.1 Laser Light Source

A 5-mw HeNe continuous-wave (CW) laser is used as the light source for the interferometer (Fig. 1). A block beam splitter with dielectric partial reflective coatings in an adjustable mount splits the laser beam into two beams of equal intensity. The two beams emerge from the beam splitter parallel. The separation between them is adjustable by rotating the beam splitter block. The separation of the two beams at this point controls the interferometric fringe period,  $\lambda_s$ , in the fringe zone [see Eq. (1)].

A diffraction-limited, laser-focusing lens (L1) focuses the bottom laser beam (probe beam). The probe beam diameter must be smaller than the size of the turbulent cells found in thin, supersonic boundary layers in order to obtain sufficient sensitivity to the density changes as they pass through the probe focal waist. Since knowledge of the size of the turbulent structure in supersonic boundary layers is incomplete, the beam is focused to the smallest diameter possible within the restraints of diffraction limit theory. The top half of the probe beam focusing lens was removed to permit passage of the reference beam above it. The half-lens is mounted so that its axis is raised above the laser beam axis to superimpose the probe beam over the reference beam. Here the nearly plane waves from the two beams interfere forming a fringe zone at the diffuse reflector plane located on the opposite side of the wind tunnel from the optical head.

### 2.2.2 Receiving Optics

In order to eliminate the traversing/alignment problems associated with sensing the fringe movements at this point with a slit and detector, a receiving lens (L2) in the optical head forms an image of the real fringes in the plane of the diffuse surface on the slit plane

located in the optical head. A process camera lens is used to form a sharp, high-contrast image of the fringes. The lens and this geometry provide a magnification which is within limits for process lens design for high resolution and minimal aberrations. Therefore, the fringe period at the diffuser plane is reduced by about 20 percent at the image plane. A slit width was analytically and experimentally determined to be optimum for maximum sensitivity to fractional fringe movements. The lens is used in the full-open position to reduce the size of the speckle to a minimum, thus reducing the speckle noise. Speckle width is given approximately by

$$w = 1.22 \lambda f \quad (2)$$

where  $\lambda$  is the wavelength of the laser light and  $f$  is the f/number of the lens. Angular alignment of the slit length with the fringes and sharp focus of the fringes at the slit are critical to obtaining clean a-c signals over the d-c level and other noise. A narrow bandpass filter centered at the 0.6328- $\mu\text{m}$  laser light wavelength is located between the slit and the photodetector to filter out unwanted ambient light.

### 2.2.3 Optical Signal Detection

Fluctuation in light intensity ( $\Delta I$ ) behind the slit caused by fringe movement is detected with a silicon avalanche detector, which is the solid-state equivalent to a photomultiplier tube. The silicon avalanche detector outputs a current signal proportional to the amount of optical input signal. The current signal output of this detector is fed into a pre-amplifier circuit. The pre-amplifier circuit is composed of an operational amplifier configured as a trans-impedance amplifier which outputs a voltage signal proportional to the input current signal. This current-to-voltage amplifier contains significant gain as well as high-frequency noise-filtering circuitry. The voltage signal output of the pre-amplifier stage is fed into an output line driver stage capable of providing ample signal output to several instruments. A circuit schematic diagram is shown in Fig. 2.

### 2.2.4 Signal Processing and Display

The output of the Boundary-Layer Transition Detector (BLTD) circuit is connected through coaxial lines to an analog tape recorder, a spectrum analyzer, and an RMS voltmeter. The spectrum analyzer performs frequency analysis of the input signals and displays frequency spectra in real time. Hard copies of frequency spectra are made with an X-Y plotter, which also functions as a front-end data acquisition unit for a minicomputer

system. The minicomputer system is used to control data acquisition and analysis. A functional block diagram of the BLTD and associated hardware is shown in Fig. 3.

The BLTD and associated data display and recording hardware are shown in Fig. 4. The optical head shown with the cover removed measures 8 by 8 by 34 in. and weighs 37 lb. The spectrum analyzer variable bandpass frequency filter, rms meter, and XY plotter dedicated to the BLTD are mounted in a movable rack. The minicomputer used to control the data recording and the analog magnetic tape recorder for recording the data are not shown.

### **3.0 WIND TUNNEL EXPERIMENTS**

Wind tunnel experiments were conducted in the AEDC 50-in. hypersonic Tunnel B at Mach 8 to evaluate the performance of the BLTD and to compare boundary-layer data from the BLTD with other methods of transition detection. The model was a 1-m-long, 7-deg half-angle, sharp nose cone.

#### **3.1 INSTRUMENT TRAVERSING MOUNT**

The BLTD optical head was mounted on an XY traversing mount outside the two 18-in.-diam test section windows (Fig. 5). Axial points along the surface of the model (X) were probed within the area constraints of the windows. A white diffuse surface was mounted outside the window on the far side of the tunnel to act as the viewing screen for the fringes. The BLTD optical axis was aligned perpendicular to the tunnel axis and set to the correct distance from the tunnel centerline to place the focused waist of the probe beam in the boundary layer directly over the top surface of the model. The fringes were focused on the slit by imaging the slit precisely at the diffuse surface plane.

The transition table position readout in X was calibrated to locate stations that were located in 1-in. increments from the nose of the model. The beam position above the model surface (Y) could be determined by touching the surface with the probe beam and viewing light scattered from the metal model surface. The beam was then moved up slightly to miss the model surface.

#### **3.2 EXPERIMENT PROCEDURE**

Two surveys along the top of the model in the X direction were made with the BLTD: one at a free-stream Reynolds number/ft of  $2.0 \times 10^6$  and one at  $Re/ft$  of  $3.0 \times 10^6$ . The probe beam was aligned 0.005 in. above the model surface at each station. Approximately 30

seconds of data were recorded, and a frequency spectrum was recorded on the XY plotter at each station. The frequency spectra was viewed on the analog spectrum analyzer CRT as the survey was being made, providing real-time information about the boundary layer.

### 3.2.1 Boundary-Layer Characterization

Typical flow visualization of laminar, transitional, and fully turbulent boundary-layer flow is shown in the shadowgram of a cone model in Fig. 6. The frequency spectra shown in Fig. 7 ( $\Delta I_{\text{rms}}$  versus frequency) is from three stations along the model that were selected to show the characteristic frequency spectra of laminar, transitional, and fully turbulent boundary-layer flow at  $\text{Re}/\text{ft } 2.0 \times 10^6$ . The frequency spectrum in a laminar boundary-layer station  $X = 8$  is much like that of free stream with the exception of a slight increase in  $\Delta I_{\text{rms}}$  at frequencies below 60 kHz, where  $I$  is the fringe intensity behind the slit. During the onset of transitional flow, periodic waves (usually referred to as Tollmien-Schlichting type waves or simply "roping") start to form and are transported downstream. At station  $X = 23$  where these waves are fully formed, the frequency spectrum reveals a pronounced amplitude peak in  $\Delta I_{\text{rms}}$  centered at approximately 150 kHz as shown in Fig. 7. This characteristic spectrum is very similar to spectra from hot-wire anemometry and other detection methods. An important point is that the magnitude of the sudden increase in  $\Delta I_{\text{rms}}$  when these periodic waves occur is not important to the detection of transitional flow. With this model and tunnel test conditions, these waves were detectable along approximately 8 in. of the model. At station  $X = 30$ , the waves have undergone line broadening, producing a broad band, random frequency spectrum which is considered to be fully turbulent flow.

Similar spectra are shown in Fig. 8 for an  $\text{Re}/\text{ft } 3.0 \times 10^6$ . Note that the frequency spectrum characteristics are the same as those at  $\text{Re}/\text{ft } 2.0 \times 10^6$  (Fig. 7). However, note that the transitional waves have moved toward the nose of the model at the higher Reynolds number, and the peak center frequency is higher, which was predicted from theory and past data (Ref. 1).

### 3.2.2 Comparison of BLTD Data

A comparison of the BLTD data was made with other transition detection methods used on this test, i.e., shadowgraph, hot-wire anemometry, and heat-transfer gages in the model. All of the techniques agreed as to the location of transition along the model even though the measurements were not made simultaneously. A comparison between the BLTD and hot-wire frequency spectra is shown in Fig 9.

Figure 10 is a compilation of the location of transition on the 7-deg cone model using several independent detection methods. Transition location at  $Re/ft\ 2.0 \times 10^6$  is shown on the top model surface and at  $Re/ft\ 3.0 \times 10^6$  on the bottom model surface. Considering that the Tollmien-Schlichting waves are present over several inches of the model surface at these tunnel flow conditions, the data agree very well even though the measurements were not made simultaneously.

The wavelength of the Tollmien-Schlichting waves was measured from the shadowgrams and used with the frequency of the waves measured with the BLTD to calculate flow velocity. These velocities were in nominal agreement with velocities inferred from pitot tube measurements in the boundary layer. Surveys made perpendicular to the model surface indicate a higher level of turbulent activity ( $\Delta I_{rms}$ ) from 0.075 to 0.100 in. above the surface, which corresponds with the maximum disturbance energy point found with the hot-wire probe under the same conditions.

#### 4.0 CONCLUSIONS

A new method has been developed using a variation of laser interferometer whose fringe phase shifts caused by turbulence can be quantitatively linked to boundary-layer transition. Boundary-layer data recorded with the BLTD on various model shapes from Mach 4 to Mach 8 agree with previously recorded data, theoretical Tollmien-Schlichting wave predictions, and other standard methods of boundary-layer characterization. The BLTD offers an alternative to techniques that require expensive fabrication of expendable probes, are intrusive to the flow field, require model modifications or surface preparation, and are time consuming to install, calibrate, and operate. Results to date indicate additional capabilities may exist with further experimentation and additional signal-processing capabilities.

#### REFERENCES

1. Nickell, J. C. and Demetriades, Anthony. "Evaluation of Boundary Layer Transition Sensors in a Hypersonic Wind Tunnel Environment." *Instrumentation in the Aerospace Industry*, Vol. 27, Proceedings of the 27th International Instrumentation Symposium, Indianapolis, Indiana, April 27-30, 1981, pp.631-652.
2. Holly, Sandor. "Lateral Interferometry—Its Characteristics, Technology, and Applications." *Optical Engineering*, Vol. 15, No. 2, March-April 1976, pp. 146-150.

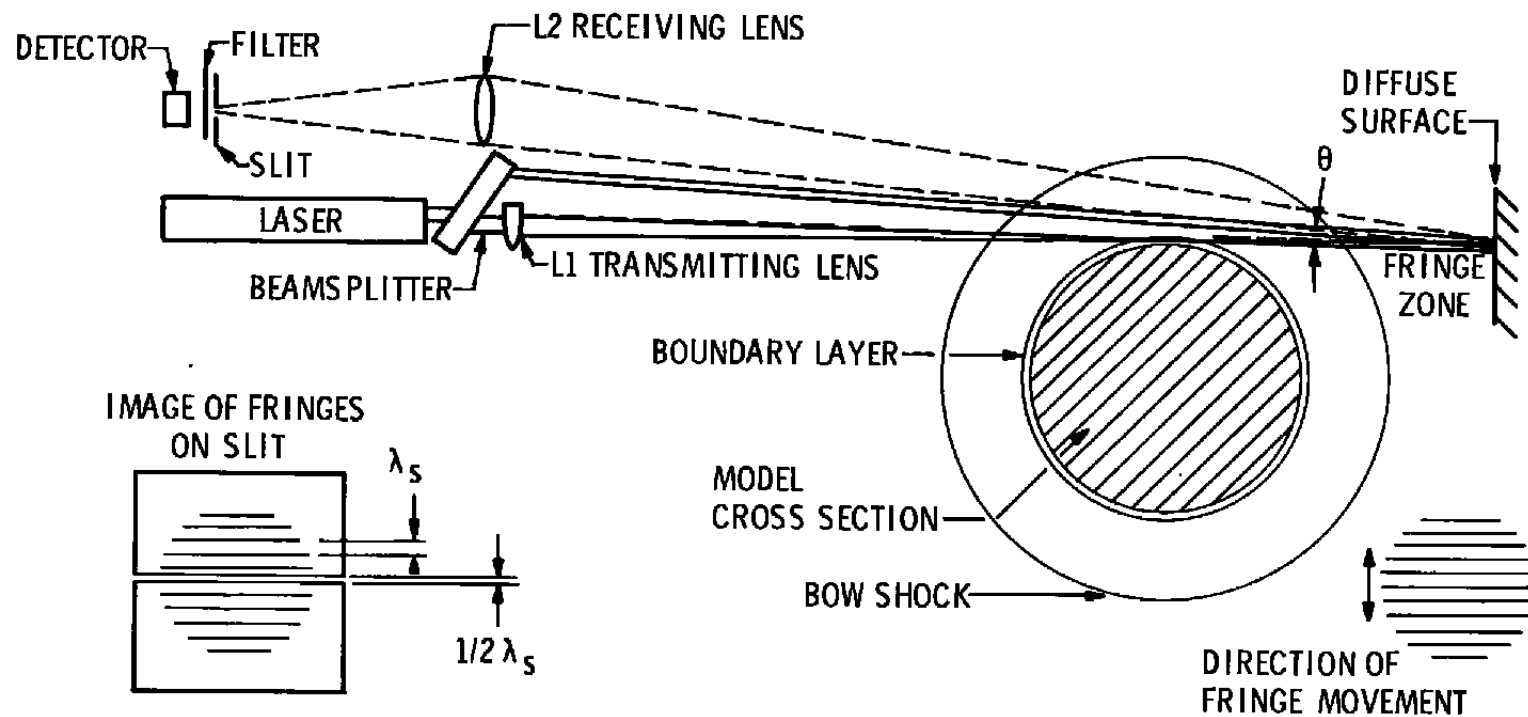


Figure 1. Schematic of boundary-layer transition detector.

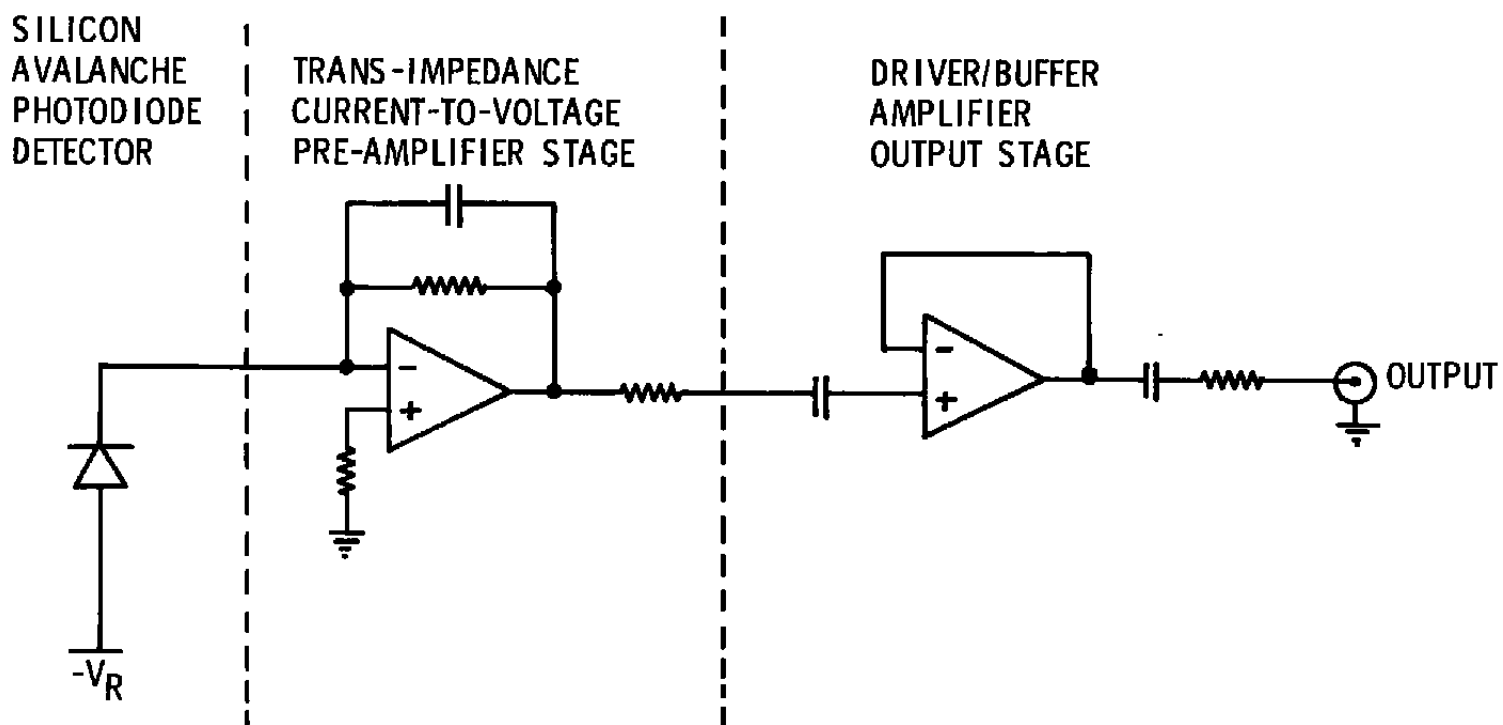


Figure 2. Boundary-layer transition detector and signal conditioning schematic.

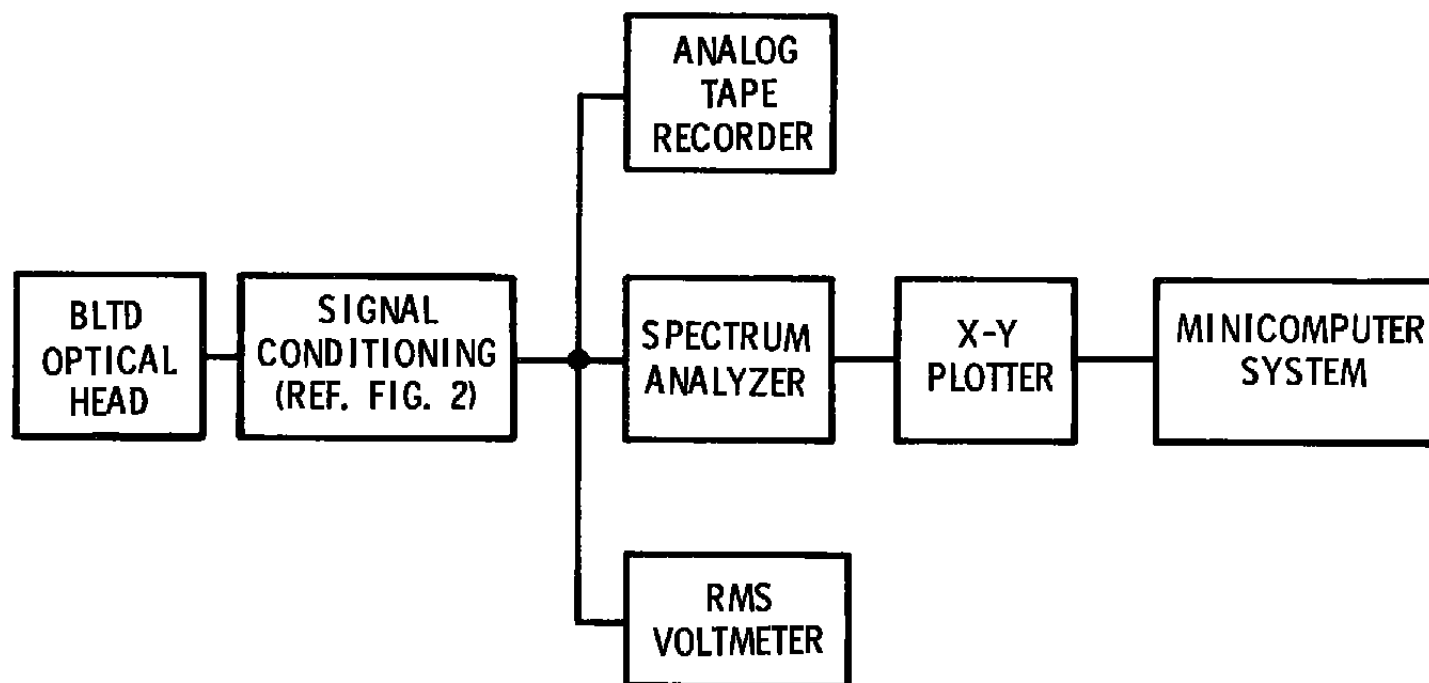
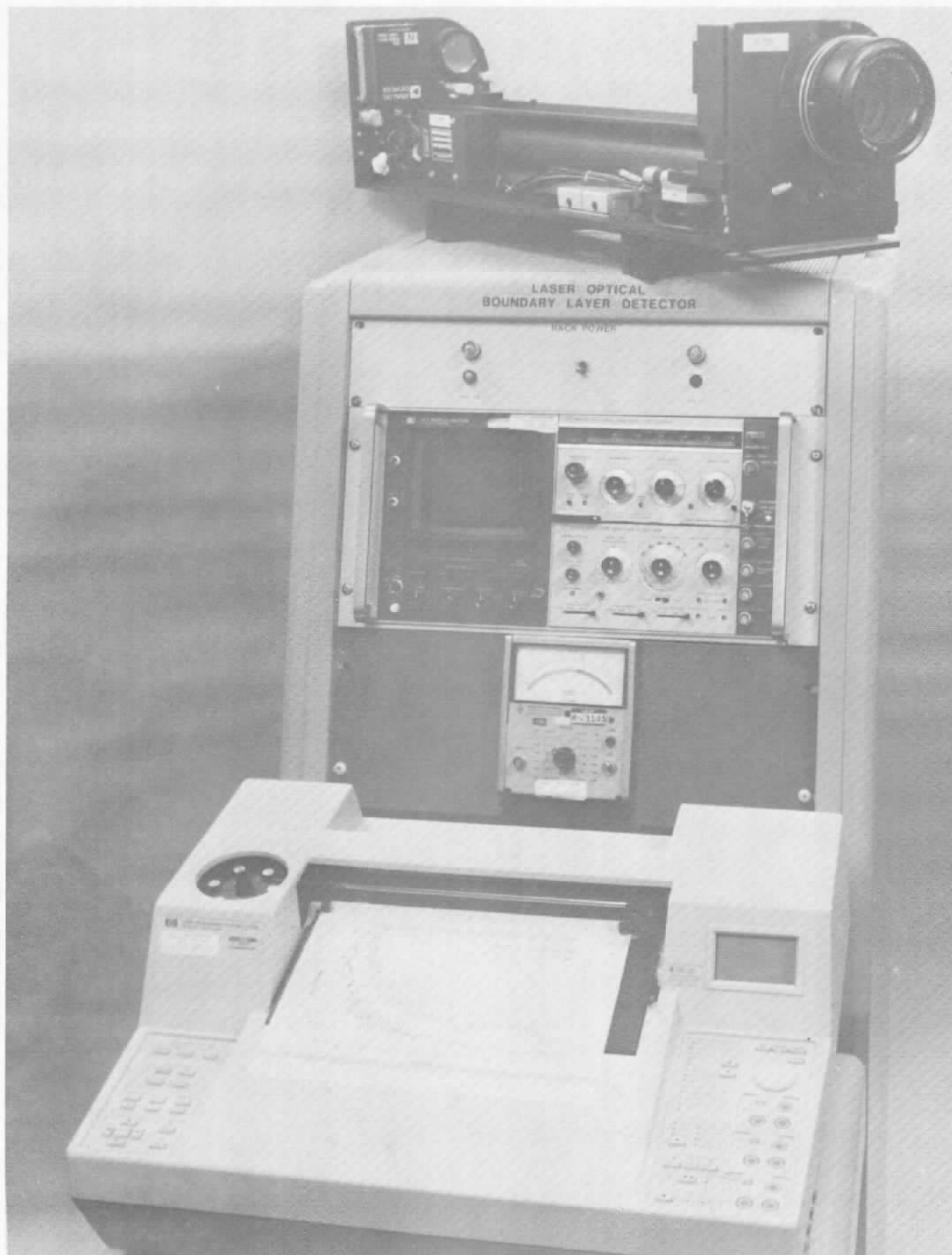


Figure 3. Boundary-layer transition detector system hardware.





**Figure 4. Boundary-layer transition detector optical head and data recording system.**

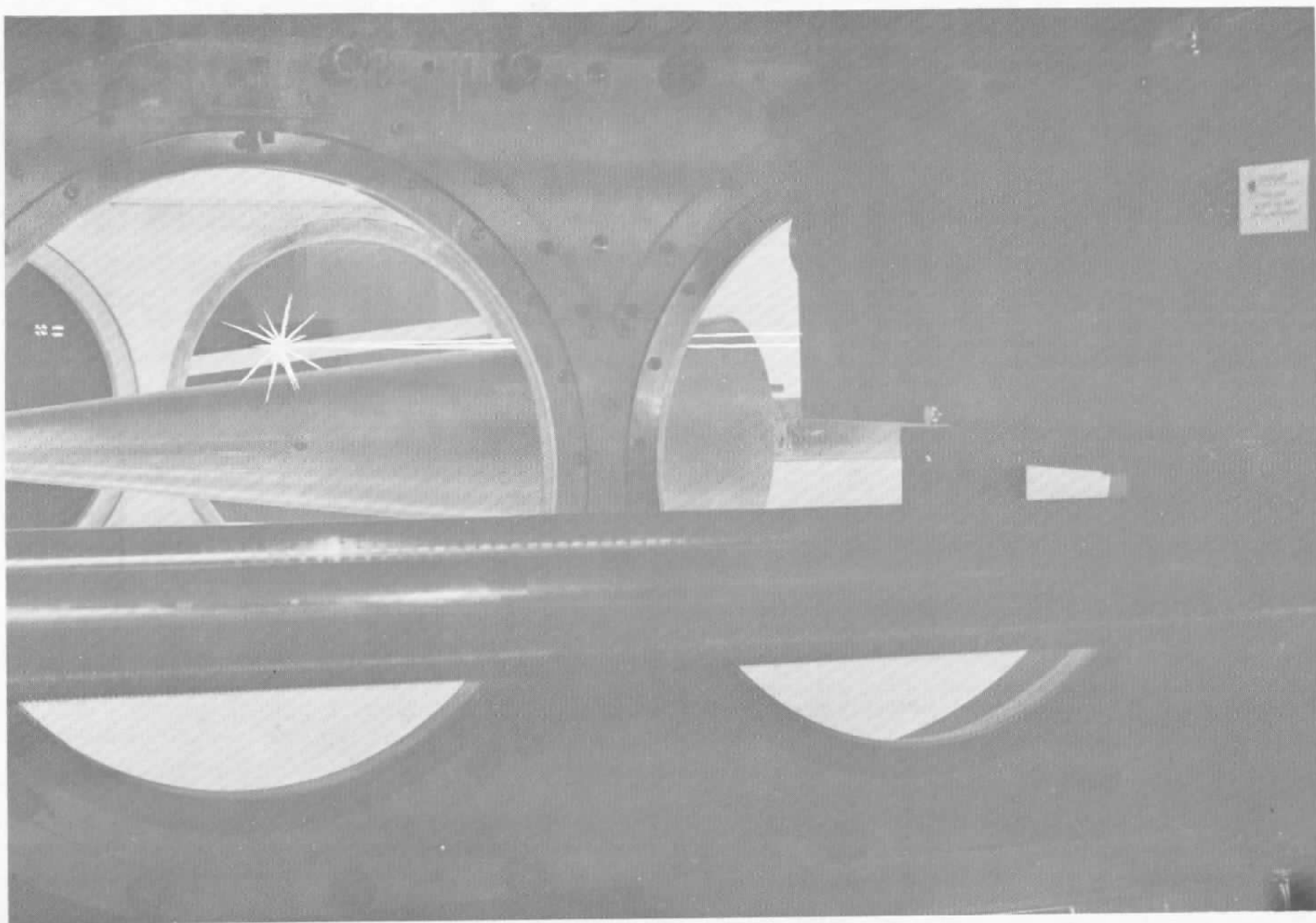


Figure 5. Boundary-layer transition detector and cone model installed in AEDC hypersonic tunnel B.

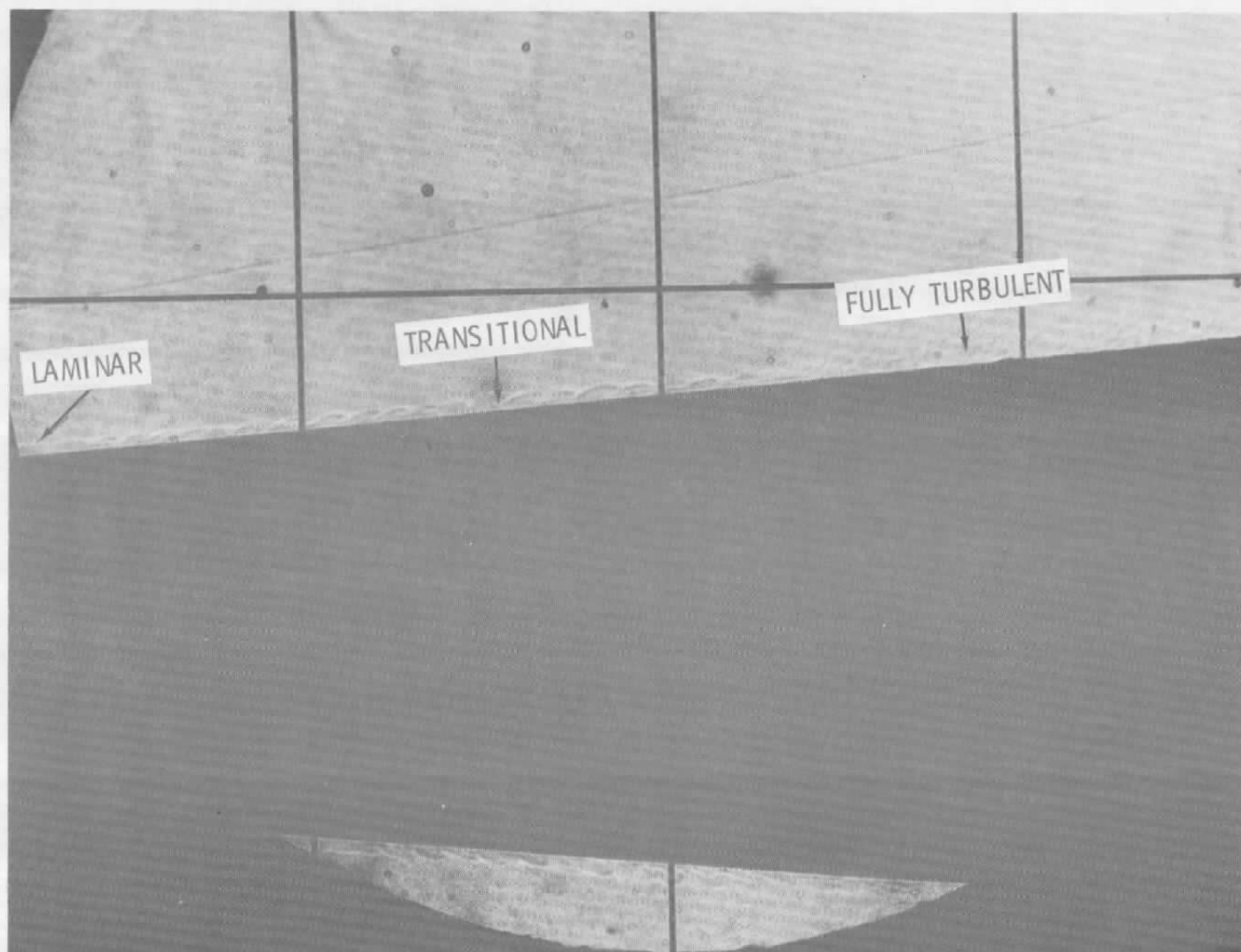


Figure 6. Shadowgram of laminar, transitional, and fully turbulent boundary-layer flow.

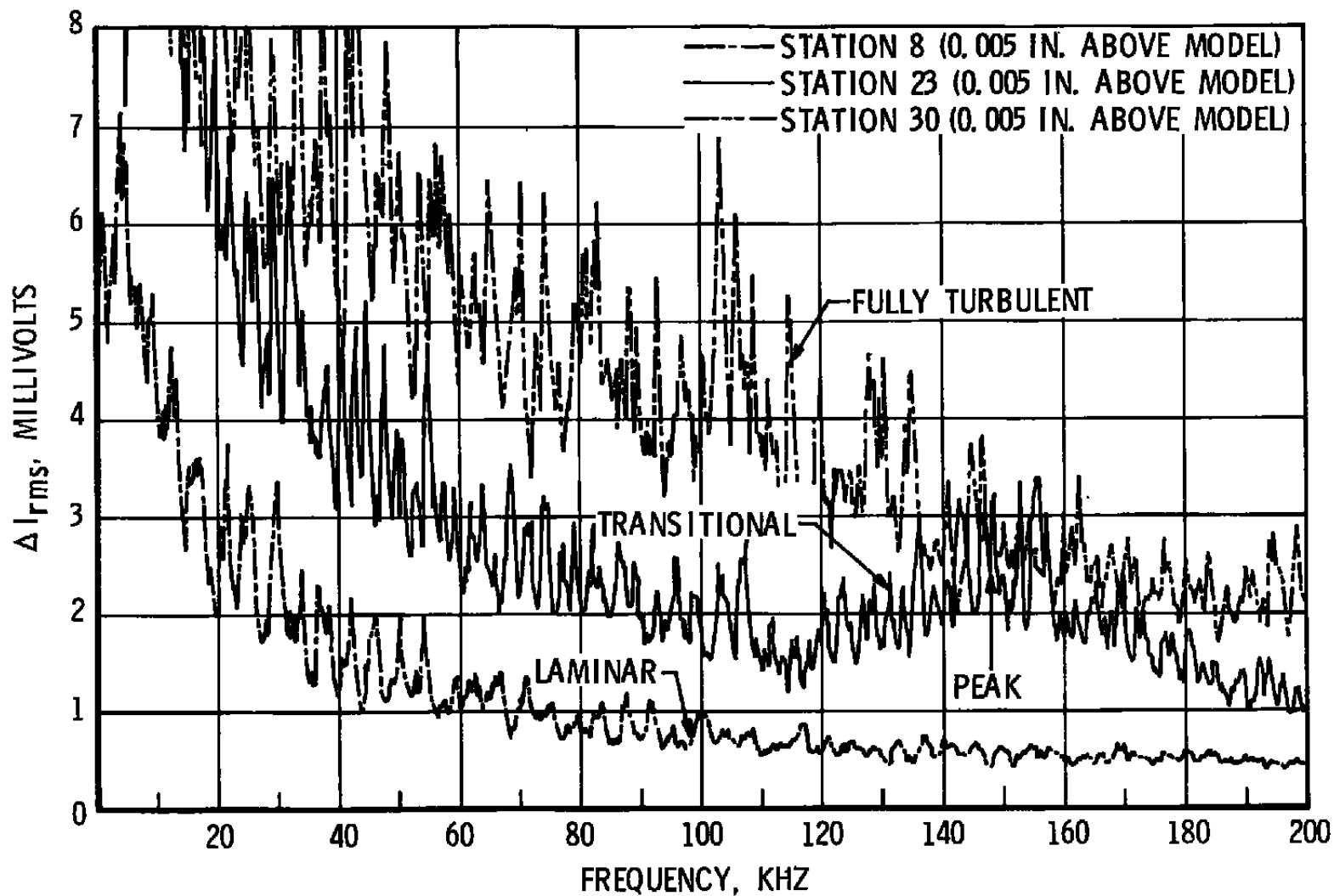


Figure 7. Boundary-layer survey, 7-deg cone, Mach 8, Re/ft  $2.0 \times 10^6$ .

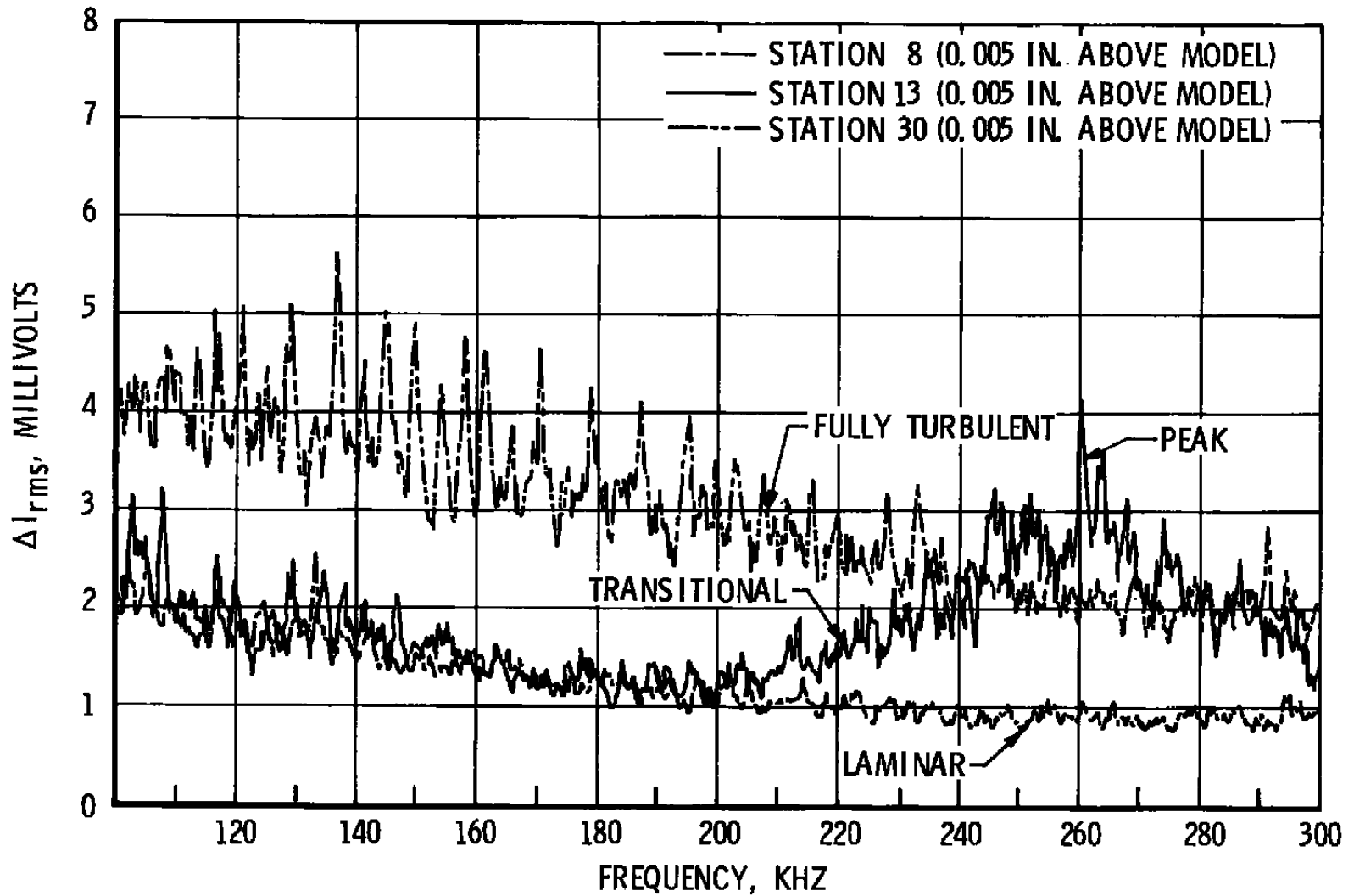


Figure 8. Boundary-layer survey, 7-deg cone, Mach 8,  $Re/ft\ 3.0 \times 10^6$ .

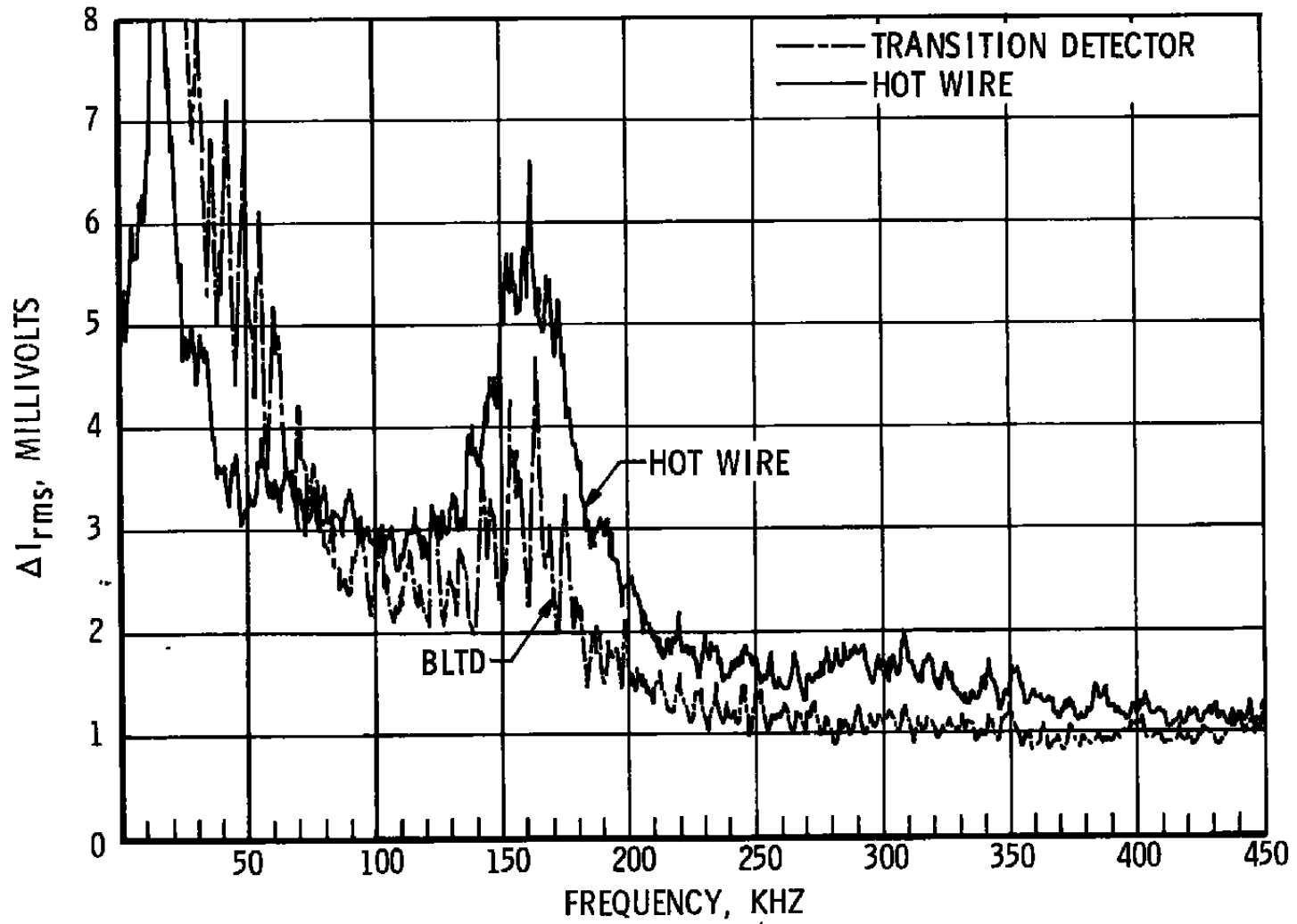


Figure 9. Comparison of BLTD and hot-wire spectra, Mach 8,  $Re/ft\ 2.0 \times 10^6$ , station X = 13.

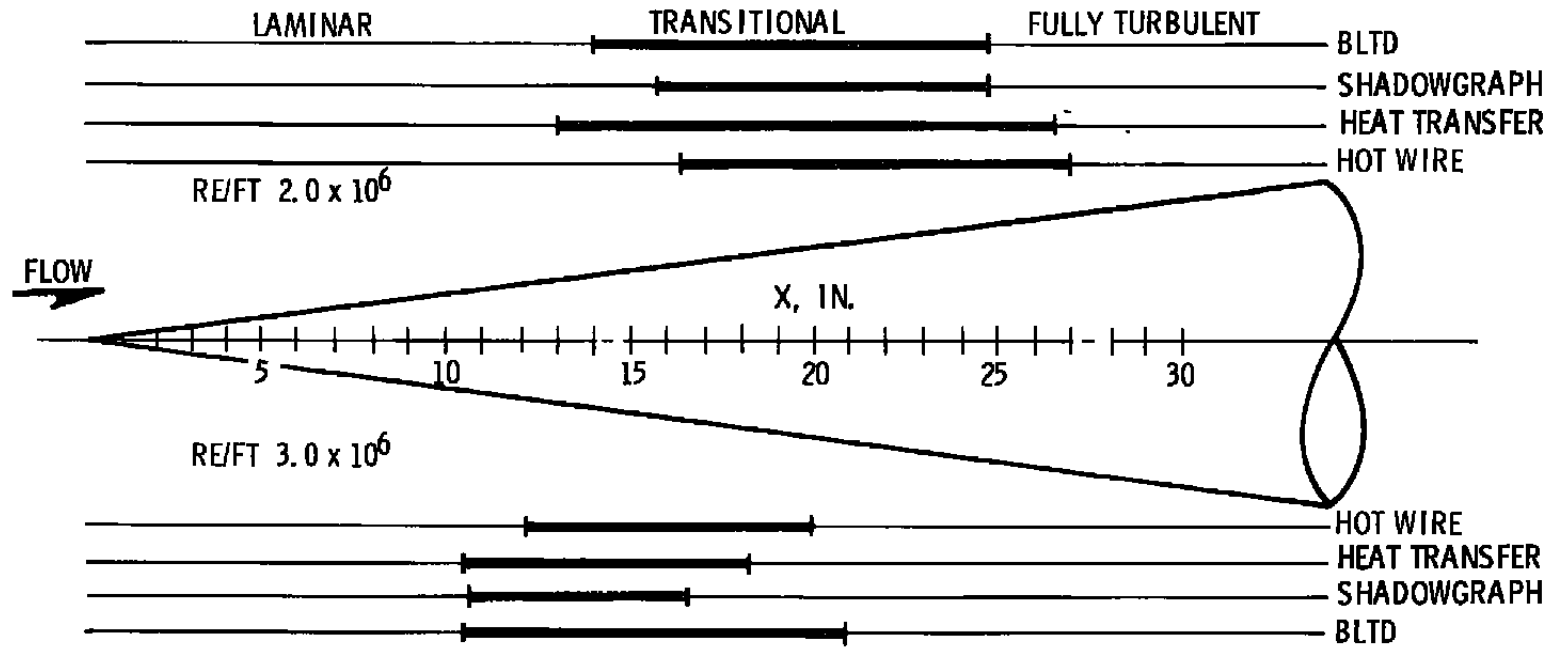


Figure 10. Boundary-layer transition on a 7-deg cone at Mach 8.